Letters

A Self-Compensated Planar Coil With Integrated Single-Switch Regulator for Wireless Power Transfer (WPT) Systems

Young-Dal Lee, Keon-Woo Kim, and Gun-Woo Moon, *Member, IEEE*

***Abstract*—In the receiver-side (R_X) of the wireless power transfer (WPT) system, the R_X is composed of compensation capacitors, a rectifier stage, and a dc/dc stage. Among them, the compensation capacitors are an essential component to minimize reactive power. Also, the dc/dc stage is an inevitable component to supply a stable output to the battery. However, to meet these aforementioned unavoidable requirements, a large number of components are required in R_X of the WPT system, which increases the overall system size and cost. To relieve these drawbacks, a self-compensated planar coil with integrated single-switch regulator for the WPT system is proposed in this letter. The proposed converter can remove the many number of compensation capacitors by utilizing the intrinsic capacitance between adjacent layers of the planar coil as a self-compensated factor. Moreover, by integrating a single-switch into the rectifier stage, it is possible to supply a stable output to the battery with only a single power stage and low cost. Besides, the proposed structure can obtain reduced switching loss by securing the soft-switching operation under the rated load condition. The effectiveness of the proposed structure is verified experimentally by a prototype under 150V_{DC} input and 60 W/33 V output.**

***Index Terms*—Integrated regulator, planar coil, self-compensated, single-stage, WPT systems.**

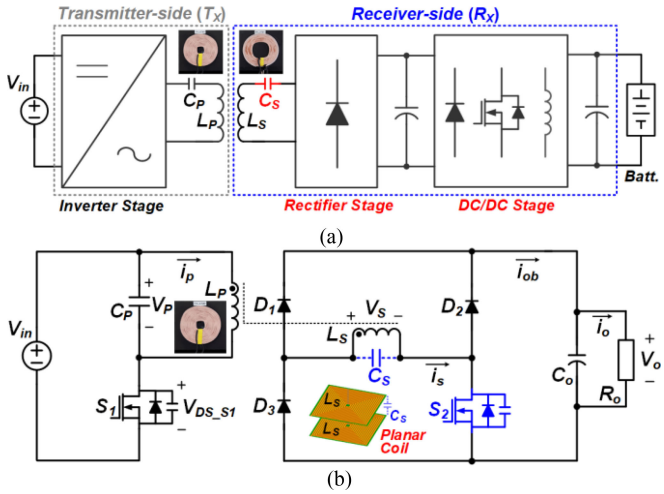

Fig. 1. Conventional and Proposed WPT structure. (a) Conventional WPT structure. (b) Proposed self-compensated integrated regulator structure.

I. Introduction

RECENTLY, the demand for wireless power transfer (WPT) systems has been exploded due to the convenience of use in many applications [1]. Accordingly, the development of such WPT system has been actively investigated [2]–[6]. One of the key objectives for the WPT system development is to achieve compact size and low cost.

Meanwhile, Fig. 1(a) shows the conventional structure for the WPT system. A conventional WPT system is composed of a transmitter-side (T_X) and a receiver-side (R_X). Among them, the R_X serves to supply a stable output to the back-end battery. As shown in Fig. 1(a), the conventional R_X has many number of components and power stages: compensation capacitors, a rectifier stage, and a dc/dc stage. Here, compensation capacitors are essential components to minimize reactive power. Next, the role of the rectifier stage is to convert the ac power from the T_X to dc power.

Also, the main purpose of the R_X is to supply a stable output voltage V_O to the back-end battery. In order to supply stable output to the back-end battery, an inevitable dc/dc stage should be required between the rectifier stage and the back-end battery. Therefore, R_X of the WPT systems require large overall system size and high cost because there are many number of components such as compensation capacitors and two power stages [2]. So as to overcome the shortcomings of the conventional R_X structure, many research works using the semiactive rectifier (SAR) structure has been actively conducted [2]–[5]. This SAR structure has advantages such as a simple structure, and low voltage stress of all devices which is clamped to the output voltage V_O. However, it is difficult to have an attraction in terms of low cost and high reliability, because the SAR structure has to utilize active components of two switches. In addition, most of the existing studies [2]–[5] have been approached by only integrating the two power stages of the receiver-side: the rectifier stage and the dc/dc stage. Also, in case of compensation capacitor, there are only few research works to eliminate physical capacitor [6].

Manuscript received November 10, 2020; revised December 23, 2020 and February 12, 2021; accepted March 1, 2021. Date of publication March 17, 2021; date of current version June 30, 2021. This work was supported by the National Research Foundation of Korea grant funded by the Korea government (MSIP) (2019R1A2B5B02070509). *(Corresponding author: Gun-Woo Moon.)*

The authors are with the Korea Advanced Institute of Science and Technology, Daejeon 34141, Korea (e-mail: youngdal.lee@kaist.ac.kr; rainbowdot@kaist.ac.kr; gwmoon@kaist.ac.kr).

Color versions of one or more figures in this article are available at https://doi.org/10.1109/TPEL.2021.3066413.

Digital Object Identifier 10.1109/TPEL.2021.3066413

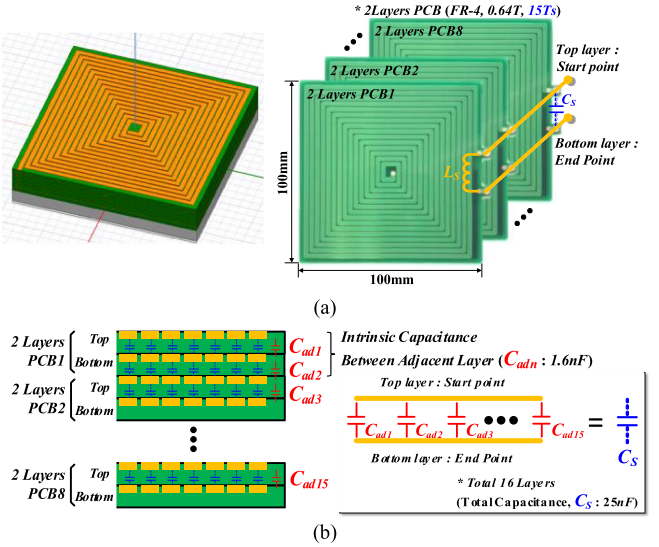

Fig. 2. R_X planar coil prototype. (a) Maxwell simulation model and fabricated planar coil. (b) Intrinsic capacitance between adjacent layers.

In this letter, a self-compensated planar coil with integrated single-switch regulator for the WPT system is proposed as shown in Fig 1(b). Since the proposed structure utilizes the intrinsic capacitance (C_S) between adjacent layers of the planar coil as a compensation capacitor, it is possible to save the volume occupied by the compensation capacitor in the conventional R_X structure.

Moreover, the proposed structure takes only a single power stage by integrating single-switch S_2 into the rectifier as shown in Fig. 1(b), thus, it is possible to supply stable output to the battery without an inevitable dc/dc stage. Besides, in the proposed structure, the integrated single-switch S_2 can obtain the soft-switching operation such as zero voltage switching (ZVS) turn-ON with contributing to reduced switching loss of the WPT system.

II. Analysis of the Proposed Converter

A. Self-Compensated Effect With Planar Coils

In the proposed structure, the method of obtaining the capacitance as compensation capacitors is to use the intrinsic capacitance generated between two adjacent layers by matching the square shape pattern as shown in Fig. 2(b). When using a square shape pattern for planar coil as shown in Fig. 2(a), it is possible to acquire a higher capacitance compared to using a circular shape pattern under the same space. It means that the resonance frequency can be operated within the range of tens to hundreds kilohertz, which is a more usable range rather than an absurdly high megahertz This can easily prove the distance (d: 0.235∼0.240 mm), area (A: 8992 mm^2), and permittivity of two dielectrics with FR-4 (ε: 4.8∗8.854 pF/m with FR-4) through a following general equation ($C_{ad} = \varepsilon A/d = 1.66$ nF).

Moreover, in the simulation results by using the Maxwell simulator from ANSYS Inc., the capacitance of the square shape pattern can be improved by approximately 30% compared to

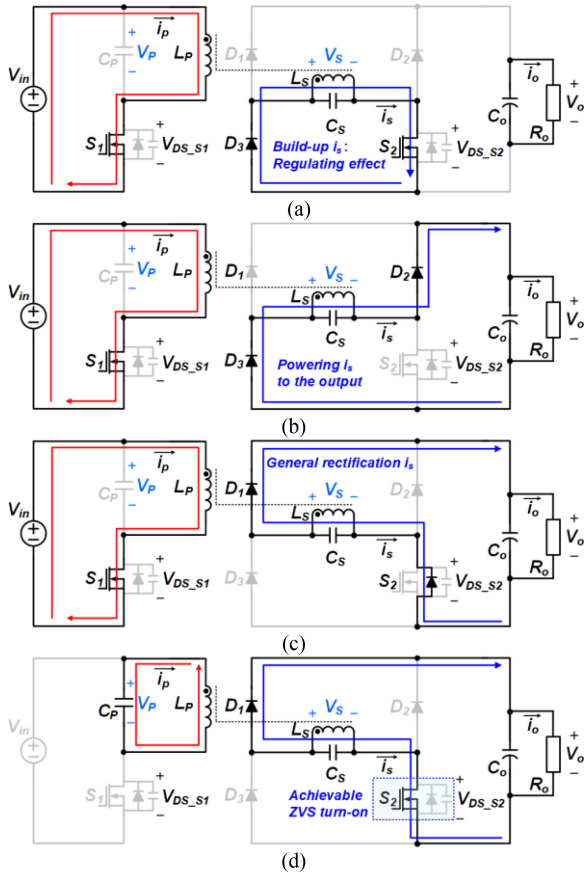

Fig. 3. Operational mode of the proposed integrated regulator. (a) Mode 1(t_0∼t_1). (b) Mode 2(t_1∼t_2). (c) Mode 3(t_2∼t_3). (d) Mode 4(t_3∼t_4).

the circular shape pattern. If a square shape pattern coil is utilized, the higher capacitance can be achieved than circular shape pattern. Therefore, in this letter, a square shape pattern coil is proposed by considering switching frequency. Besides, in the proposed structure, the square shape patterns for the planar coil are connected in parallel to ensure high intrinsic capacitance C_S. Thus, the obtainable capacitance can be expressed by the following:

$$C_S = \sum_{k=1}^{n-1} n \cdot C_{adn} \text{ here, } (n = 2m - 1). \tag{1}$$

Here, "m" means the total number of two layers PCB (m = 8), and "n" means the number of capacitances by adjacent layers (n = 15). That is, a total of 15 capacitances are generated between the generated layers (C_{ad1}∼C_{ad15}). Therefore, it is possible to obtain a self-compensated effect by utilizing these capacitances (C_{ad1}∼C_{ad15}) as a compensation capacitor C_S.

B. Mode Analysis of the Proposed Regulator

In this section, the operational principle of the proposed converter is going to be explained based on Figs. 3 and 4.

Mode 1 [t_0∼t_1*]:* In this interval, the switches S_1 and S_2 are simultaneously turn-ON state. The proposed structure creates a special interval in which two switches are simultaneously turned

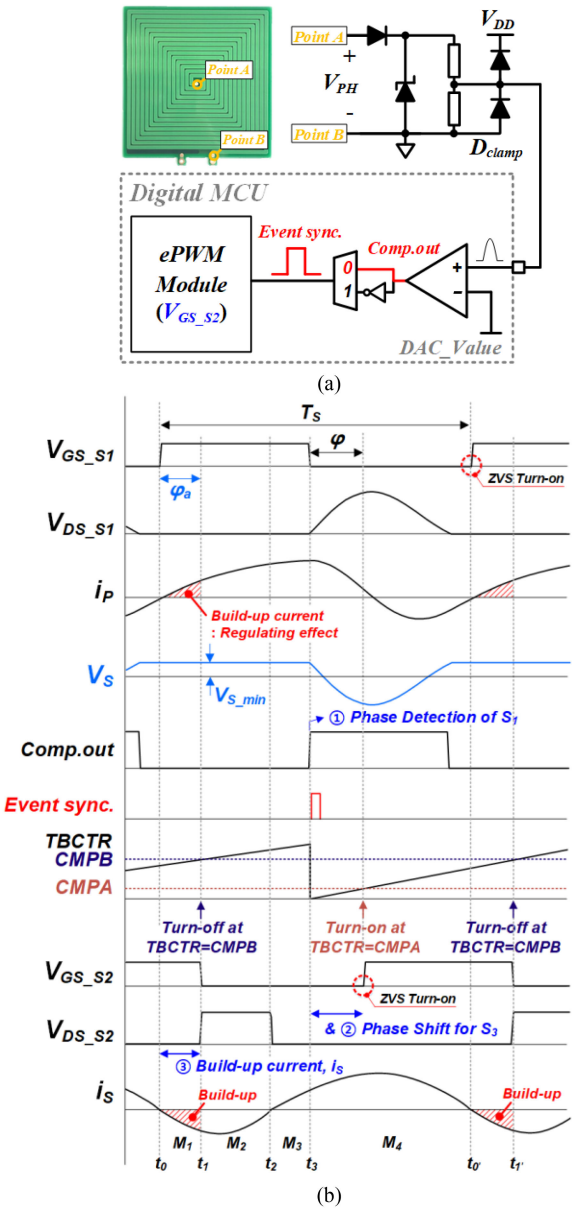

Fig. 4. Control of the proposed converter. (a) Phase-shift control circuit diagram. (b) Key waveforms and of the proposed converter.

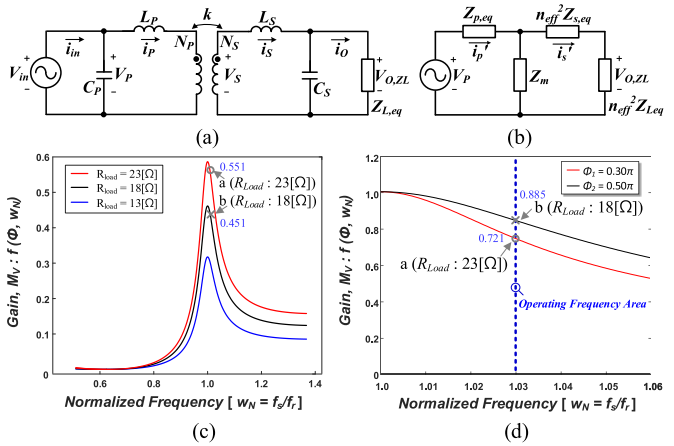

Fig. 5. Gain characteristics of the proposed converter under the rated loads and normalized frequency ($w_N = f_s/f_r$). (a) Equivalent lumped circuit model. (b) Simplified model. (c) Gain Curve of Impedance vs. w_N. (d) Gain curve of phase-shift Φ_a versus w_N.

ON by the phase-shift operation. When the switches S_1 and S_2 are turned ON at the same interval, the build-up of T_X current i_P is created as shown in Fig. 3(a). In other words, according to the load condition, this build-up current i_P is used as a regulation factor to adjust the output voltage V_O.

Mode 2 [t_1~t_2]: The next mode starts when the switch S_2 is turned OFF at t_1. And then, build-up current i_P in the previous mode 1 delivers energy to the output through diodes D_2 and D_3. This interval performs as a general powering operation.

Mode 3 [t_2~t_3]: At the time t_2, the next mode starts when the polarity of the R_X current i_S is changed. Through diode D_1 and the body diode of switch S_2, the energy is transferred to the final output. As the R_X current i_S conducts through the body diode of switch S_2, the ZVS condition of S_2 is created.

Mode 4 [t_3~t_4]: This mode starts when the switch S_1 is turned OFF. The C_P & L_P resonate with charging and discharging the junction capacitor of switch S_1. Through this operation, ZVS turn-ON for switch S_1 is achievable. In addition, switch S_2 is also turned ON while satisfying the ZVS condition through the conduction path of the previous mode 3.

C. Control Method of the Proposed Regulator

The control method of the proposed regulator is as follows.

As shown in Fig. 4(b), in order to acquire phase-shift operation for the R_X switch S_2 based on phase information of the T_X switch S_1, the simple phase sensing method is required as shown in Fig. 4(a). Through the "*Point A*" and "*Point B*" in the top side of the planar coil in Fig. 4(a), the phase information of the T_X switch S_1 can be easily obtained without complex calculation. The V_{PH} is the (+) terminal input of the internal comparator inside the digital MCU, and an arbitrary DAC value is input to the (−) terminal and finally "*comp.out*" signal is generated as shown in Fig. 4(a). At the rising edge of this "*comp.out*" signal, the synchronized "*event.sync*" signal is created. With the "*event.sync*" signal, phase-shift operation of the R_X switch S_2 is adjusted according to the load variation.

Furthermore, equalizing the proposed converter as in Fig. 5(a), define current i_p' and i_s' on each node as in Fig. 5(b). Finally, the gain characteristic of the proposed converter is expressed by (2) with the voltage distribution rule of each impedance shown in Fig. 5(a). Through (3), the gain of the proposed converter is dependently changed by the load equivalent resistance $Z_{L,eq}$. Also, $Z_{L,eq}$ changes according to the amount of build-up current that varies depending on the phase-shift operation (Φ_a) as shown in Fig. 4(b).

When the load resistance is 23 Ω, the load is lower than the rated load condition, thus, in this case, the gain of the converter increases as shown in Fig. 5(c). In order to compensate for this characteristic, the proposed converter narrows the phase (0.3π)

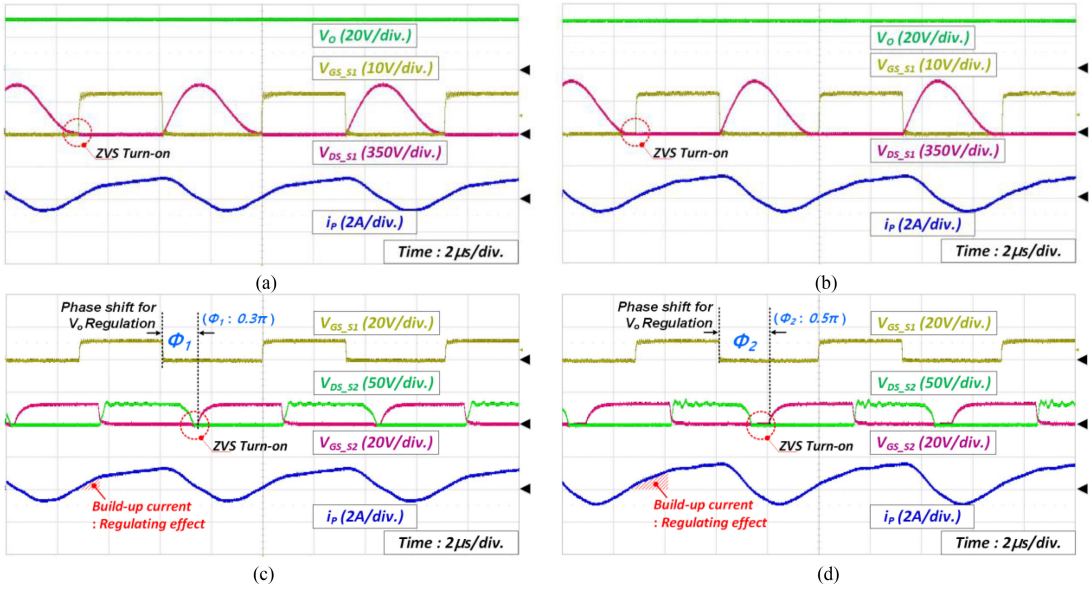

Fig. 6. Experimental waveforms of component voltage stress: (a) under 23 Ω load; (b) under 18 Ω load; (c) under 23 Ω load; and (d) under 18 Ω load.

as shown in Figs. 5(d) and 6(c)

$$M = \frac{V_{O,ZL}}{V_P} = \frac{1}{Z_{P,eq} + Z_m \parallel (n_{eff}{}^2 Z_{S,eq} + n_{eff}{}^2 Z_{L,eq})} \cdot \frac{Z_m}{Z_m + n_{eff}{}^2 Z_{S,eq} + n_{eff}{}^2 Z_{L,eq}} \cdot n_{eff}{}^2 Z_{L,eq} \quad (2)$$

$$Z_{L,eq} = \frac{v_s}{i_s} = \frac{4}{\pi^2} \cdot R_L(1 - \cos(\varphi_a)) \cdot e^{j(\pi)}$$

$$\text{here, } \varphi_a = \varphi - t_{\text{deadtime}}. \quad (3)$$

III. Experimental Results

Based on the former analysis, the feasibility of the proposed converter has been verified by experimental results with a prototype under $150V_{DC}$ input and 60 W/33 V output. The switching frequency is 140 kHz in consideration of the resonant frequency of the two coils and resonant capacitors. The detailed parameters regarding the main components and experimental test configurations are listed in Table I.

Fig. 6 shows the steady-state waveforms of the proposed structure according to the load variation. When the converter is under the heavy load 18 Ω condition, the gain of the converter can be decreased. To compensate for this, the proposed converter gradually shifts (0.5π) the turn-ON time of S_2 compared to the switch S_1 with stable output.

Fig. 7 shows the measured efficiency with the Yokogawa WT-2000 power analyzer under load variation. The maximum output is at 60 W when the load is 18 Ω as shown in Fig. 7. It has more than 75% efficiency in most load conditions. This tendency is due to soft-switching such as ZVS turn-ON for both switches S_1 & S_2 as shown in the waveforms of Fig. 6(c) and (d).

TABLE I
Design Parameters of Proposed Structure

Components	Parameters Description
Input	$150V_{DC}$
Output	60W/33V
f_{sw}	140kHz
L_P (General Coil)	590μH (0.1Φ*80strands, 101Ts)
L_S (Planar Coil)	56μH (Pattern width : 2.5mm, 2oz, 15Ts)
Planar Coil Size	100 x 100 x 0.64 mm^3
Vertical Distance	10mm
C_P (Compensation Cap.)	2.2nF
C_S (Intrinsic Cap.)	25nF
Planar Coil Size	100 x 100 x 0.64 mm^3
Pri. Switch	S_1 : C3M0065090D (900V, 65mΩ, 66pF)
Sec. Switch	S_2 : IPP020N06N (60V, 2.0mΩ, 1800pF)
Rect. Diodes	D_1~D_3 : V40100C (100V, V_F = 0.67)

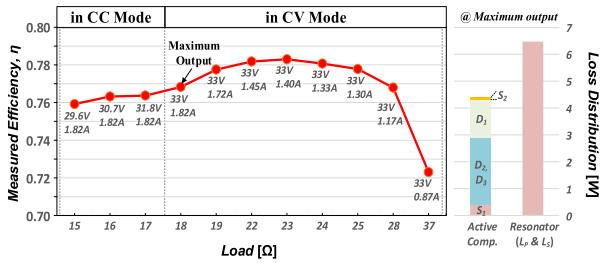

Fig. 7. Measured efficiency according to the load variation.

IV. Conclusion

In this letter, a self-compensated planar coil with integrated single-switch regulator for the WPT system is proposed. Since the proposed structure utilizes the intrinsic capacitance (C_S) between adjacent layers of the planar coil as a compensation capacitor, it is possible to save the volume by the compensation

capacitor in the conventional R_X structure. Moreover, the proposed structure takes only a single power stage by integrating a single-switch into the rectifier, it is possible to supply stable output to the battery without an inevitable dc/dc stage. Besides, in the proposed structure, as all the switches S_1 & S_2 can acquire the soft-switching operation such as ZVS turn-ON with reduced switching loss. Therefore, the proposed structure is expected to contribute to the reduced size and low cost of the R_X for the WPT system.

REFERENCES

[1] S. C. Moon and G. W. Moon, "Wireless power transfer system with an asymmetric four-coil resonator for electric vehicle battery chargers," *IEEE Trans. Power Electron.*, vol. 31, no. 10, pp. 6844–6854, Oct. 2016.

[2] K. Colak, E. Asa, M. Bojarski, and D. Czarkowski, "A novel phase-shift control of semibridgeless active rectifier for wireless power transfer applications," *IEEE Trans. Power Electron.*, vol. 30, no. 11, pp. 6288–6297, Nov. 2015.

[3] T. Mishima and E. Morita, "High-frequency bridgeless rectifier based ZVS multiresonant converter for inductive power transfer featuring high-voltage GaN-HFET," *IEEE Trans. Ind. Electron.*, vol. 64, no. 11, pp. 9155–9164, Nov. 2017.

[4] Z. Huang, C. Lam, P. Mak, R. Martins, S. Wong, and C. Tse, "A single-stage inductive-power-transfer converter for constant-power and maximum-efficiency battery charging," *IEEE Trans. Power Electron.*, vol. 35, no. 9, pp. 8973–8984, Sep. 2020.

[5] I. Iam *et al.*, "Constant-frequency and non-communication-based inductive power transfer converter for battery charging," *IEEE J. Emerg. Sel. Top.Power Electron*, to be published, doi 10.1109/JESTPE.2020.3004259.

[6] J. Li and D. Costinett, "Analysis and design of a series self-resonant coil for wireless power transfer," in *Proc. Appl. Power Electron. Conf. Expo.*, 2018, pp. 1052–1059.